Environmental Science & Technology

pubs.acs.org/est

Article

River Winds and Transport of Forest Volatiles in the Amazonian Riparian Ecoregion

Jianhuai Ye, Carla E. Batista, Tianning Zhao, Jesus Campos, Yongjing Ma, Patricia Guimarães, Igor O. Ribeiro, Adan S. S. Medeiros, Matthew P. Stewart, Jordi Vilà-Guerau de Arellano, Alex B. Guenther, Rodrigo Augusto Ferreira de Souza, and Scot T. Martin*

Cite This: https://doi.org/10.1021/acs.est.1c08460

Read Online

ACCESS | Metrics & More | Article Recommendations | Supporting Information

ABSTRACT: Volatile organic compounds (VOCs) emitted from forests are important chemical components that affect ecosystem functioning, atmospheric chemistry, and regional climate. Temperature differences between a forest and an adjacent river can induce winds that influence VOC fate and transport. Quantitative observations and scientific understanding, however, remain lacking. Herein, daytime VOC datasets were collected from the surface up to 500 m over the "Rio Negro" river in Amazonia. During time periods of river winds, isoprene, α-pinene, and β-pinene concentrations increased by 50, 60, and 80% over the river, respectively. The concentrations at 500 m were up to 80% greater compared to those at 100 m because of the transport path of river winds. By comparison, the concentration of methacrolein, a VOC oxidation product, did not depend on river winds or height. The differing observations for primary emissions and oxidation products can be explained by the coupling of timescales among emission, reaction, and transport. This behavior was captured in large-eddy simulations with a coupled chemistry model. The observed and simulated roles of river winds in VOC fate and transport highlight the need for improved representation of these processes in regional models of air quality and chemistry−climate coupling.

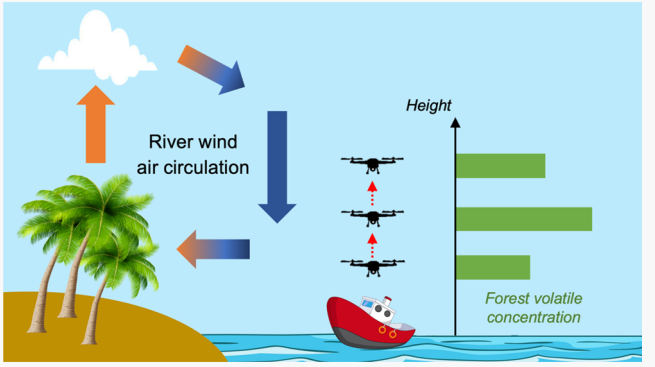

KEYWORDS: *volatile organic compounds, river wind, riparian ecoregion, Amazon tropical forest, unmanned aerial vehicle*

Downloaded via UNIV OF CALIFORNIA IRVINE on July 27, 2022 at 18:55:01 (UTC).
See https://pubs.acs.org/sharingguidelines for options on how to legitimately share published articles.

1. INTRODUCTION

The Amazon ecosystem, comprising the single largest hydrographic basin on earth, plays indispensable roles in the exchange of energy, water, and gases between the biosphere and the atmosphere on regional and global scales.[1−3] Around 15% of the Amazon basin is covered by freshwater landscapes, constituting an open water area of rivers of 10^5 km^2 across the basin.[4] The Amazon basin holds a substantial number of the world's longest and widest rivers, such as the Amazon, Madeira, Negro, and Tapajos rivers.[5] Large rivers are important elements in the coupling between land and atmospheric processes in the Amazon. The coupling has significant impacts on atmospheric fate and transport of chemical species and regional climate.[6−10]

The river environment serves as a unique ecoregion of flora and fauna within the Amazon biome.[8,10−13] A distinct distribution of cloudiness is induced via river−land−atmosphere interactions,[14,15] and photosynthetically active radiation and temperature are altered. As a result, the mix of species in the flora of the riverbank region and their atmospheric emissions shift relative to the surrounding forest, including net ecosystem carbon exchange.[8,10] This riparian ecoregion and its emissions are further influenced by local environmental stresses, such as flooding and drought. For instance, isoprenoid emissions from seedlings of several widely distributed tree species, such as *Garcinia macrophylla* and *Hevea spruceana* in várzea and igapó, which are two typical floodplains in the central Amazon, decrease by more than 50% when waterlogged.[11] In contrast, the emission of green leaf volatiles can significantly increase under drought stress, as a result of high leaf temperatures that induce senescence and the loss of net carbon assimilation.[12,13] These green leaf volatiles and other volatile organic compounds (VOCs) emitted from the forests are important species connecting the biosphere and the atmosphere, especially in the Amazon region. Released into the atmosphere, these biogenic VOCs also strongly affect atmospheric chemistry and regional climate over the Amazon,

Received: December 14, 2021
Revised: May 10, 2022
Accepted: May 12, 2022

© XXXX American Chemical Society

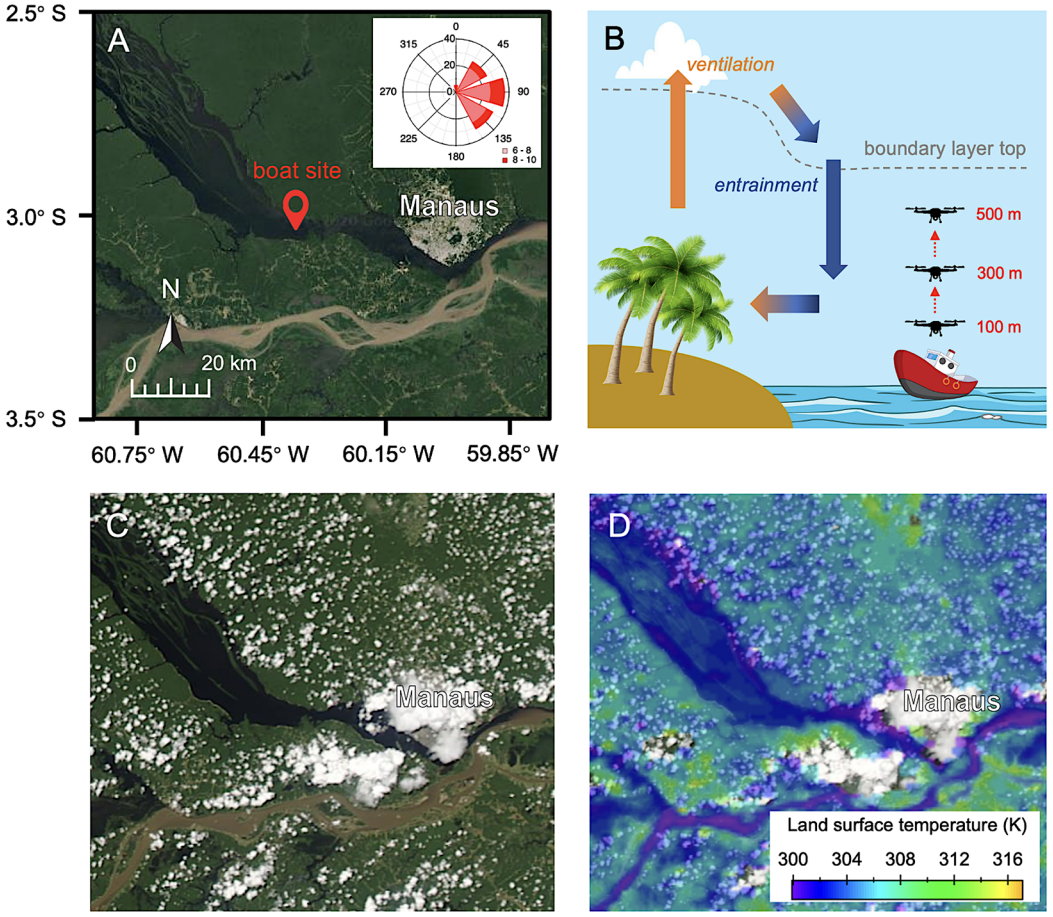

Figure 1. (A) Location of the observation site (3.0708° S, 60.3604° W) in the middle of the Rio Negro River and 35 km to the west of Manaus city. Image credit: Google Earth. The inset shows the wind rose measured at 500 m by the UAV during the measurement periods. The figure is for the subset of data characterized by wind speeds greater than 6 m s^{-1} to capture times of trade winds. The wind rose is consistent with typical reports in the literature for the same region.[41] (B) Conceptual layout of the river winds and UAV sampling over the Rio Negro. (C) Satellite imagery on 26 September 2019 at 13:30 (AMT) in the presence of river winds. (D) Satellite mapping of surface temperatures during the same period. Image credit: NASA's Earth Observatory.

in part because they are critical precursors of ozone and particulate matter.[2,3]

Thermally driven local circulations in the form of river winds are one of the most important atmospheric processes induced by Amazon rivers in the first few hundred meters of the overlying atmospheric boundary layer.[8,10,15−17] Like sea and lake breezes, river winds are driven by temperature differences across earth surfaces in a river−forest landscape. In the daytime, higher land temperatures and lower river temperatures lead to convective turbulent ascent of air parcels over the land and to corresponding subsidence over the river. As a result, there is a tendency for onshore air movement from the river toward the land, and a local air circulation cell can develop in the vertical plane. At night, the land cools much more rapidly than the river, and the altered thermal contrast can reverse the local air circulation cell. For an ideal circulation cell, horizontal wind direction reverses by around 180° between the lower and higher levels of the circulation cell.[18] Large flat expanses like seas and lakes favor ideal conditions. Rivers, however, typically occur within landscapes of complex local topography. Amazon rivers of 5 to 10 km in width are neither so wide that ideal conditions exist nor so narrow that they do not perturb the local atmospheric structure and physics.[15] Thus, the resulting river winds and possible circulation cells over the Amazon rivers are a product of a complex interplay of physics that include synoptic-scale winds, heterogeneous thermal contrast in the landscape, and flow over a terrain of variable roughness and height. In consequence, the strength of river winds, including their absence at times, has high variability from day to day.

River winds can strongly affect the fate and transport of local pollution. In some cases, re-circulation rather than dispersion can result. Trebs et al.[19] carried out a boat-based campaign close to the confluence of the Rio Negro River (hereafter, "Rio Negro") and the Solimões River, two large rivers that converge to form the Amazon River near the city of Manaus (Amazonas, Brazil). In that study, a change of local wind direction occurred in the afternoon due to river winds. There was an associated doubling to quintupling in light scattering from atmospheric particulate matter and increases in the concentrations of ozone (O_3) and nitrogen oxides (NO_x). The afternoon river winds carried the pollution of Manaus city to the study site in the river. Zhao et al.[15] in a companion study to the present one reported that the vertical profiles of the concentrations of carbon monoxide (CO) and total oxidants ($O_x \equiv O_3 + NO_2$) significantly changed during time periods of river winds. During those time periods, O_x-depleted air from the nearby forest (e.g., because of the reactive loss of O_3 on leaf surfaces)

https://doi.org/10.1021/acs.est.1c08460
Environ. Sci. Technol. XXXX, XXX, XXX−XXX

and CO emissions from local pollution ascended from the land and descended over the river as part of a river−forest recirculation.

Herein, the effects of river winds on the fate and transport of biogenic VOCs in the Amazon riparian ecoregion were investigated. Vertical profiles of VOC concentrations and winds were collected over the Rio Negro using equipment mounted on an unmanned aerial vehicle (UAV) during the dry season of 2019. The UAV sensing and sampling approach has been well tested and validated for atmospheric chemistry studies in the Amazon.[15,20−24] Boat-launched UAVs have high maneuverability and positional flexibility. The approach was thus well suited to the domain sizes of river winds, which historically have been little studied with in situ measurements. Unlike UAVs, the practical challenges of direct measurements over rivers are not well addressed by many other common platforms, such as towers, balloons, and aircraft.[15] In conjunction with the UAV-acquired datasets, numerical experiments using large-eddy simulations were employed to examine factors such as trade wind speed and direction that can affect the linkages between river winds and VOC fate and transport.

2. METHODS

2.1. Observation Location and UAV Flights. UAV flights were launched from a boat in the Rio Negro in the central Amazon during the dry season from 11 September to 9 October 2019 (Figure 1A,B).[15] For VOCs, sample collection took place from 23 September 2019 and thereafter. Vertical flights from the river surface up to 500 m above it were carried out. Flight details are listed in Table S1. The Rio Negro is the largest tributary to the Amazon River, and it is the world's largest blackwater river.[25] The observation site (3.0708° S, 60.3604° W) was located in the middle of the river. The width of the Rio Negro at the observation site was 5 km, and the river depth was approximately 20 m. Landcover on both sides of the river consisted of terra firme forest.[6,26] The site was 35 km to the west of Manaus city. Equatorial trade winds prevailed at most times, and the sampling site was located downwind of Manaus (Figure 1A). Manaus has a population of over two million, and it is larger by an order of magnitude than any other city in the central Amazon.

During the flights, horizontal wind speed and wind direction were recorded by using a UAV-mounted sensor system. Remote measurements from 50 to 2500 m over the river were also simultaneously performed by using a wind lidar system aboard the boat. Section S1 in the Supporting Information provides further technical information on the instrumentation and measurements.

Satellite imagery for the study time period was obtained from the *Earth Observing System Data and Information System* (USA National Aeronautics and Space Administration, NASA).[27] Maps of land surface temperature and surface reflectance were also obtained from this database (Figure 1C,D). The data and images were collected by instrumentation on the *Terra* and *Aqua* satellites, which, respectively, passed overhead at 10:30 and 13:30 (Amazon Time or AMT, UTC minus4 h).

2.2. VOC Sampling and Analysis. During the flights, a custom-built sampler mounted on the UAV collected atmospheric VOCs at different heights over the river.[22,28] This methodology of VOC collection from the atmosphere, followed by chromatographic analysis in the laboratory, was previously employed and validated for UAV launch and retrieval from a tower in a forested region to the north of Manaus.[20] In the present study, the UAV ascended from the boat and hovered at 100, 300, and 500 m for sample collection above the river. These sampling heights were selected in part based on the upper technical limit for the height of the UAV flight (i.e., 500 m) and in part based on the simulation results of Medeiros et al.[29] In that study, river winds at times perturbed wind speed and direction from the river surface up to 150 m in altitude. At each sampling height, the UAV first hovered for 30 s to stabilize the local air and then collected samples for 5 min at a sampling flow rate of 250 mL min^{-1}. The sampled air passed through VOC-adsorbing cartridges. Cartridges were analyzed by thermal desorption gas chromatography equipped with a time-of-flight mass spectrometer. Details of the sampling procedures and chemical analysis, including example chromatograms for standards and samples, appear in Section S2 (Supporting Information). The chemical measurement uncertainty was the greater of 2 ppt or 10%. An uncertainty of 15% related to VOC sampling, including uncertainties in the sampling flow rate and environmental temperature, was also estimated. The overall combined measurement uncertainty was 20%. The scale of the turbulence induced by the UAV propellers was approximately 10 m.[22,30] This scale was not significant compared to the spatial resolution of >100 m for interpretation of the measurements of this study.

2.3. Large-Eddy Simulation. Winds in a river−forest landscape were simulated using the *Dutch Atmospheric Large-Eddy Simulation* (DALES) (version 4.1).[31] Within DALES, an on-line module for chemical kinetics coupled emissions, chemistry, and transport in the atmospheric boundary layer.[32] Parameters for DALES for the Amazon environment were previously developed.[15,33−35] The simulations were performed for fair-weather conditions under clear skies in line with the favored conditions of the UAV flights and data collection. The domain size of the simulation was 60 km × 45 km × 2.5 km for the longitudinal distance in parallel to the river orientation, the transverse distance perpendicular to the river, and the height, respectively. Unless mentioned otherwise, within the domain, the surface landscape was homogeneous longitudinally but punctuated transversely by the forest (0−20 km), river (20−25 km), and forest (25−45 km). In all simulations, the VOC emissions were homogeneous across the forested part of the landscape. There were no VOC emissions from the river region. The set of simulations and their corresponding parameters are listed in Table S2. The validation of DALES physics for the study area and period was presented in the companion study[15] and is presented in Section S3 of the Supporting Information.

3. RESULTS AND DISCUSSION

3.1. River Winds and VOC Forest Emissions. The mean mixing ratio of isoprene over the river was 2.8 ppb, and the 10 and 90% quantiles around the mean mixing ratio were 0.4 and 5.8 ppb, respectively. Hereafter, the notation of $2.8|^{5.8}_{0.4}$ is used. The dataset represented 87 mixing ratios and 29 flights. The mixing ratios for α-pinene, β-pinene, and methacrolein were $0.03|^{0.09}_{0.004}$, $0.008|^{0.02}_{0.003}$, and $0.5|^{1.1}_{0.1}$ ppb, respectively (Table S3). For the same UAV-based methodology over the canopy of a plateau forest north of Manaus at a similar time of the day, the mixing ratios for isoprene, α-pinene, and β-pinene were $4.4|^{6.7}_{1.0}$, $0.1|^{0.2}_{0.06}$, and $0.05|^{0.07}_{0.03}$ ppb, respectively.[20] (Discussion and

https://doi.org/10.1021/acs.est.1c08460
Environ. Sci. Technol. XXXX, XXX, XXX−XXX

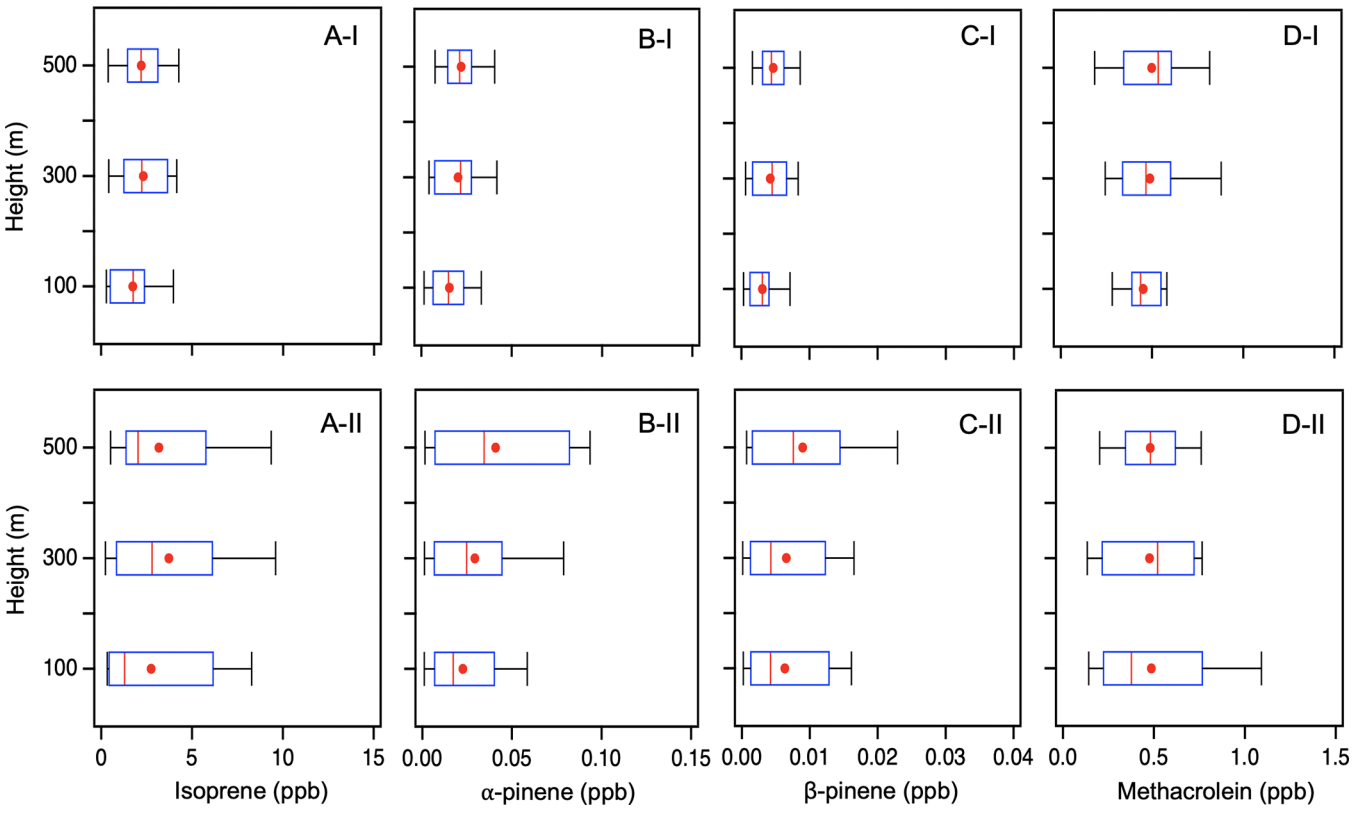

Figure 2. Box−whisker plots of VOC mixing ratios collected by the UAV at 100, 300, and 500 m above the river. (A-I,A-II) Isoprene. (B-I,B-II) α-Pinene. (C-I,C-II) β-Pinene. (D-I,D-II) Methacrolein. Panels of type "I" and "II" correspond to flights during which river winds were (I) absent or (II) present in the UAV meteorological measurements (cf. categories I and II, Tables S1 and S4). The box−whisker plot shows the minimum as the left-hand whisker, the 25% quantile as the left end of the rectangle, the median as the red line, the mean as the red dot, the 75% quantile as the right end of the rectangle, and the maximum of the dataset as the right-hand whisker.

analysis of methacrolein concentrations are presented in Section 3.2.) The mean concentrations of that prior study over the forest were thus 1.6×, 3.3×, and 6.3× higher for isoprene, α-pinene, and β-pinene, respectively, than the mean concentrations for the present study over the river. The lower means over the river compared to the earlier UAV-based forest study, and other reports for the central Amazon based on measurements just above the canopy,[36−39] can be explained by increased horizontal distance and/or greater height away from the forest source for UAV sampling over the river compared to near-field sampling over the forest.

How river winds influenced the VOC mixing ratios over the river was explored by selecting datasets from 10 UAV flights in the absence of river winds (category I in Table S1) and 10 in the presence of river winds (category II in Table S1). The presence of river winds was indicated by a reversal in wind direction between 100 and 400 m above the river (Figure S1). The methodology for identifying the occurrence of river winds was presented in our previous study by Zhao et al.[15] During time periods of river winds, the mixing ratios of each VOC species at each respective height (i.e., 100, 300, and 500 m) were all higher, compared to those time periods without river winds (Figure 2, Tables S4 and S5). The means of mixing ratios for isoprene, α-pinene, and β-pinene across all heights were greater by 50, 60, and 80%, respectively (Figure S2, Table S5). These VOCs were primary emissions from the forest, and they were not directly emitted by the river in significant quantities. The river winds advected the forest emissions from over the forest to over the river (Figure 1B), thereby increasing the mixing ratios of these species over the river landscape.

The relative importance of different factors that can affect VOC fate and transport during time periods of river winds was further examined through large-eddy simulations for several different scenarios (Table S2). For the baseline scenario (simulation 1, reference case, Table S2), the VOC lifetime was 1×10^4 s, corresponding to a typical lifetime for isoprene in a background atmosphere over a tropical forest. After methane, which is much less reactive, isoprene is the most abundant VOC emitted by tropical forests.[40]

Scenarios in the absence of strong trade winds were first examined (simulations 1 to 4, Table S2). In these simulations, the presence of a river significantly altered the distribution of the isoprene mixing ratio (Figure 3A vs 3B). For heights of 100 to 400 m over the riverbank, the mixing ratio decreased by 50% compared to the value over the forest, shifting from 4 to 2 ppb (Figure 3C). The decrease was over 90% near the surface (<100 m) and higher in the atmosphere (>600 m). The profiles at different locations around the river, specifically at the riverbank, at one-quarter across the river, and in the middle of the river, had in common lower mixing ratios at 100 m compared to higher mixing ratios at 300 and 500 m.

This low-to-high sequence of simulated mixing ratios from 100 to 500 m was consistent with the UAV-based observations. For instance, for isoprene, α-pinene, and β-pinene, the respective increases in mean mixing ratios from 100 to 500 m were 15, 80, and 40% (Figure 2). In addition, the simulated and observed occurrences of maximum VOC mixing ratios at

https://doi.org/10.1021/acs.est.1c08460
Environ. Sci. Technol. XXXX, XXX, XXX−XXX

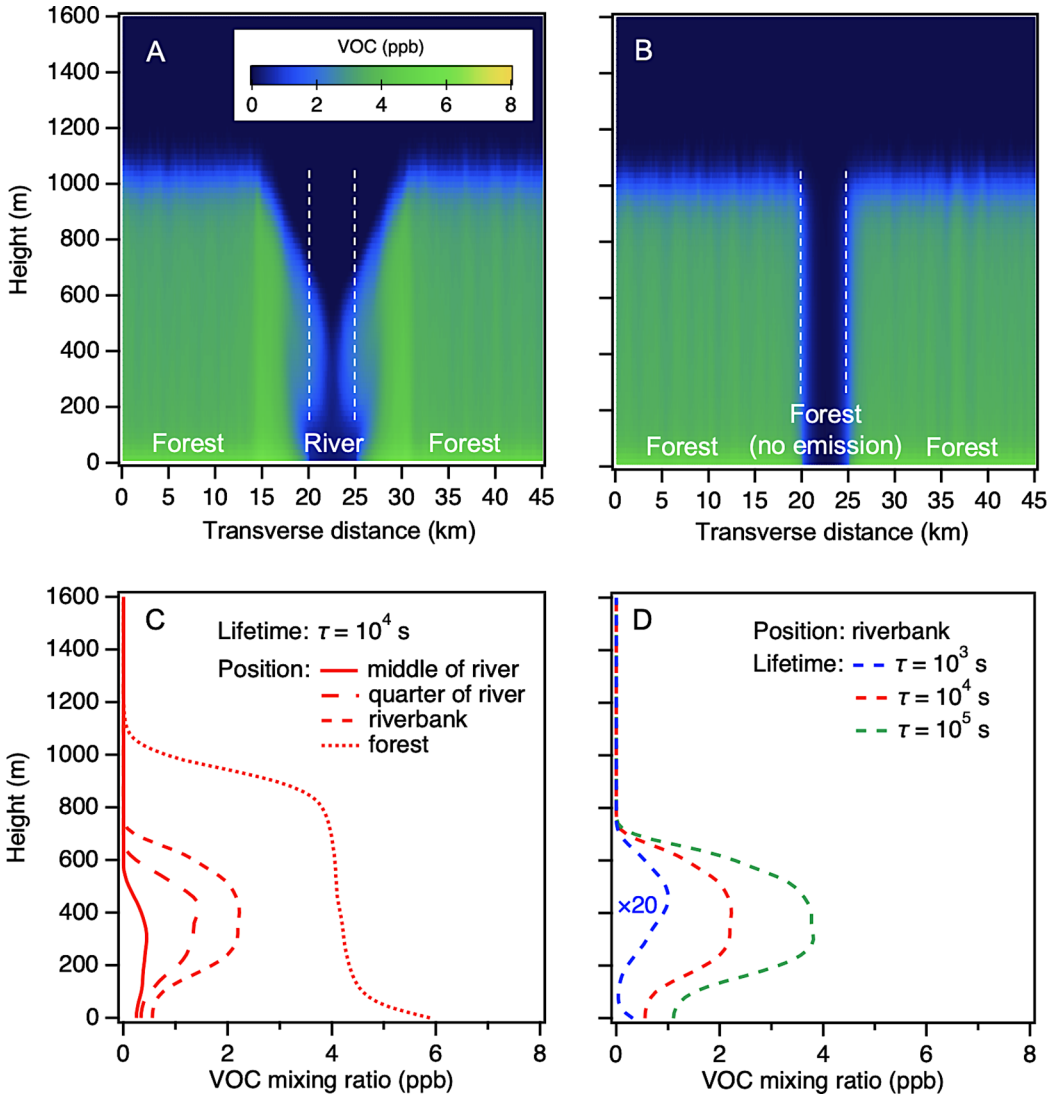

Figure 3. Simulated VOC mixing ratios for a vertical cross section that is transverse to the river orientation. (A) Reference case of river winds in a river−forest landscape (simulation 1). (B) Identical case of physical and meteorological parameters except for a fully forested landscape (simulation 2). In both panels A and B, VOC emissions are absent over the central portion, meaning a river in simulation 1 or a hypothetical section of non-emitting forest in simulation 2. Trade winds are also absent for both simulations. (C) Vertical profiles of simulated VOC mixing ratios over different locations along the abscissa of panel A. The locations labeled in the legend as the middle of the river, the quarter of the river, the riverbank, and the forest correspond, respectively, to 22.50, 27.25, 25.00, and 35.00 km along the abscissa of panel A. The lifetime τ against the chemical reaction of the VOC is 10^4 s for this panel. (D) Vertical profiles of the simulated VOC mixing ratio for lifetimes of 10^3, 10^4, and 10^5 s. Other simulation conditions are for the reference case. The mixing ratio profile for 10^3 s is scaled by 20-fold for better visualization. The location of the profile is over the riverbank, as defined for panels A and C.

mid-altitudes (Figures 2 and 3C, Table S2) also coincided with the simulated and observed height at which wind direction reversed in the presence of river winds (Figures S1B and S3C). The simulation thus captured the qualitative behavior of the vertical profiles in the datasets for VOCs. These features of VOC concentration distribution over the river atmosphere caused by river winds remain the same for VOCs of various atmospheric lifetimes (Figure 3D). An extension of these findings is that the mixing ratios of the directly emitted VOCs over the river could serve as in situ chemical tracers, in complement to meteorological data, to indicate the presence and the strength of river winds.

Scenarios in the presence of strong trade winds parallel to the river direction were also examined. For synoptic-scale trade winds that were parallel to the river landscape and over longitudinally homogeneous land surfaces (simulations 5−6), the effect of trade wind speed on the vertical distribution of mixing ratios was not significant (Figures 4A,B and S4A). For longitudinally heterogeneous land surfaces, however, parallel trade winds had important effects (simulations 7−8). Figure 4C provides an example. A forest landscape was placed upwind of the river, and the river winds were largely suppressed over the river area adjacent to the upwind forest. This suppression occurred because warm air transported from the upwind forest to over the river decreased the thermal gradient between the river surface and the surrounding riparian areas. For a trade wind speed of 2 m s^{-1}, a longitudinally upwind forest affected downwind river winds for 30 km [Figure 4(C2)]. The range of downwind effects scaled linearly with the speed of the trade winds, decreasing to 15 km for 1 m s^{-1} (Figure S4B).

These downwind effects can at least partly explain the variability in VOC mixing ratios between time periods of weak

https://doi.org/10.1021/acs.est.1c08460
Environ. Sci. Technol. XXXX, XXX, XXX−XXX

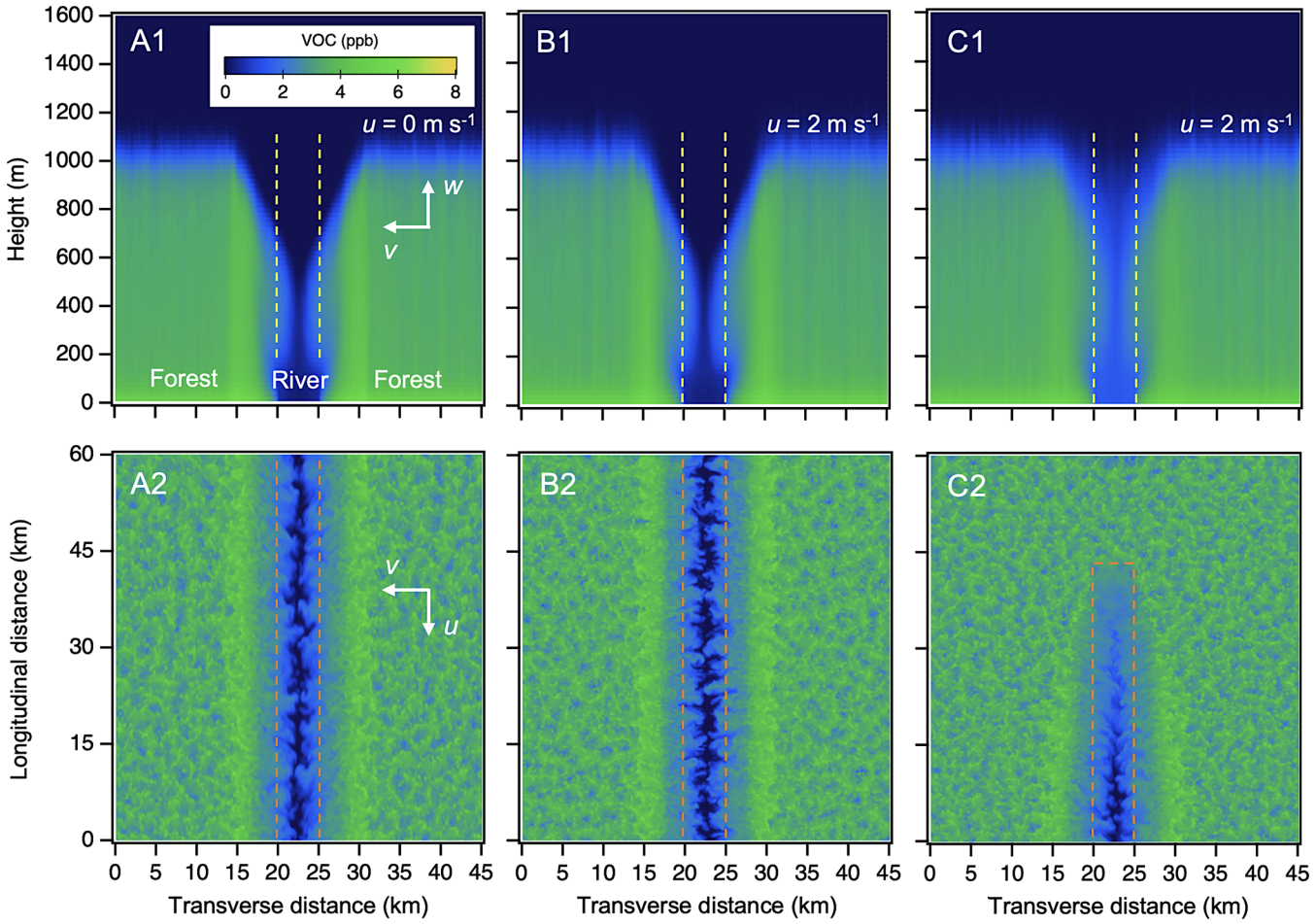

Figure 4. Interaction between river winds and trade winds. The trade winds are parallel to the river orientation. Simulated VOC mixing ratios are plotted. (A1,B1,C1) Vertical cross section in a transverse orientation to the river. The river comes out of the page. The yellow lines delineate the geographic boundaries between the river and the forest. Panel A corresponds to the reference case in the absence of trade winds (simulation 1, Table S2). Panel B includes trade winds of 2 m s^{-1}, and all other parameters are unchanged (simulation 5). Panel C evaluates a possible role of land surface heterogeneity (simulation 8). See further in panel C2 and in the main text. (A2,B2,C2) Horizontal cross section at a constant height above the river. The simulated VOC mixing ratios are averaged across a height interval of 300 to 400 m. The river is below the page. The orange lines represent the river boundaries in the underlying landscape.

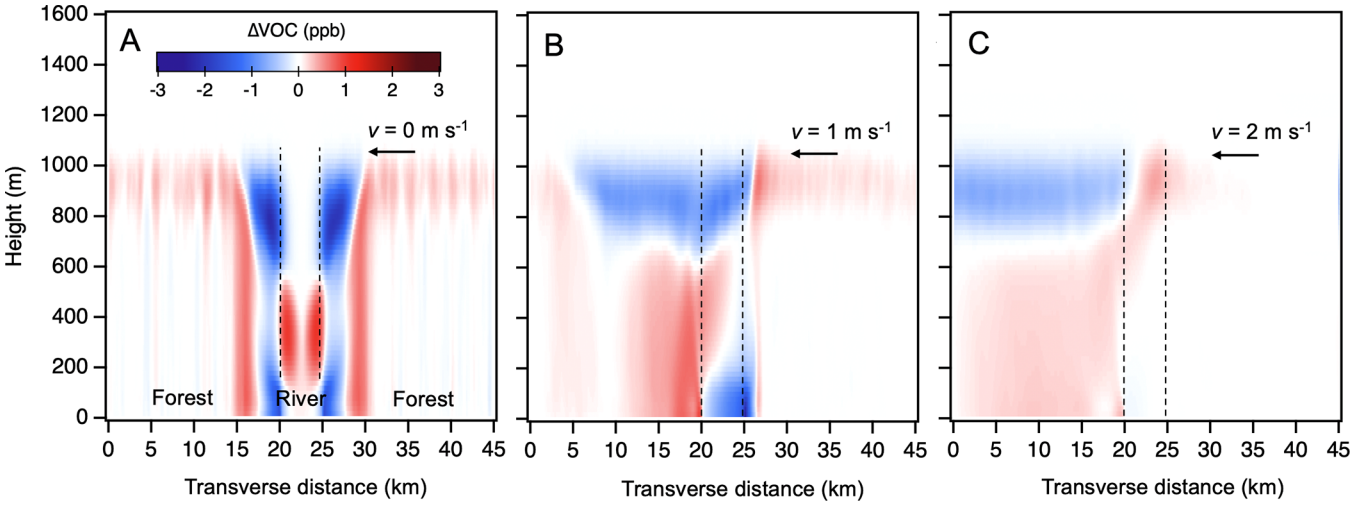

Figure 5. Interaction between river winds and trade winds. The trade winds are perpendicular to the river orientation. Difference quantities ΔVOC of simulated VOC mixing ratios are plotted. (A−C) Vertical cross section of the difference in the VOC mixing ratio between a river−forest simulation and a non-emitting all-forest simulation (simulations 1, 2, and 9−14, Table S2). Trade winds of 0, 1, and 2 m s^{-1} apply to panels A−C, respectively. A further description of the non-emitting all-forest simulation is provided in the caption of Figure 3B and in the main text.

https://doi.org/10.1021/acs.est.1c08460
Environ. Sci. Technol. XXXX, XXX, XXX−XXX

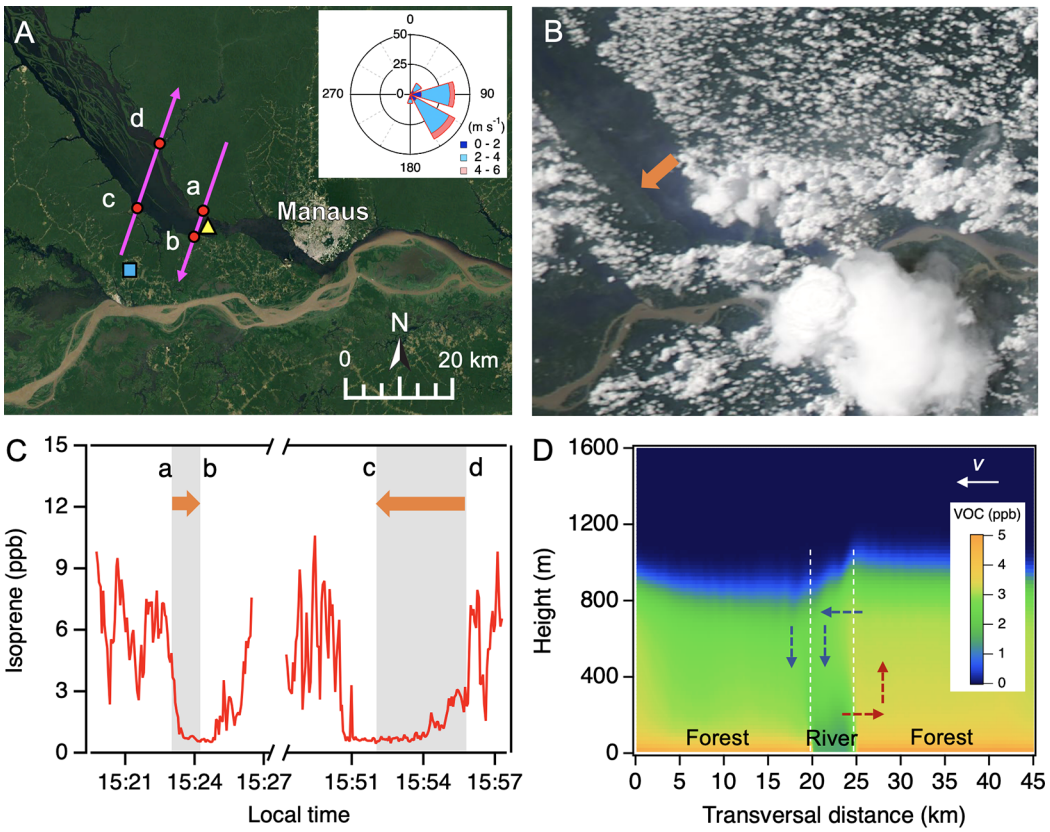

Figure 6. VOC observations by aircraft in the same geographic region as the present study but for the dry season of 2014. (A) Flight tracks at 500 m from 15:00 to 16:00 (AMT) on 18 September 2014 during GoAmazon2014/5.[3] The pink arrows show the direction of the aircraft flight. The red points show river−land boundaries along the flights. The yellow triangle shows the location of UAV launch in the present study. The inset shows the ground-level wind rose collected at the "T3" terrestrial supersite of the GoAmazon2014/5 experiment. The blue square shows the location of the T3 site. (B) Satellite images on 18 September 2014 at 13:30 (AMT). The weather was fair, and the trade winds were weak (2.6 ± 0.9 m s^{-1}, mean ± one-σ deviation). (C) Isoprene mixing ratios measured by using a proton-transfer-reaction mass spectrometer on board the aircraft. The shading indicates time periods during which the aircraft was located over the river. The corresponding distribution of the α-pinene mixing is plotted in Figure S6. (D) Vertical cross sections of VOC mixing ratios ($\tau = 10^4$ s) for simulation 10 (Table S2). The arrows represent the directions of the trade wind (white solid arrow) and the river winds at the upper and lower levels of the recirculation cell (red and blue dashed arrows). For panels A and C, the lowercase letters correspond to the same underlying riverbank locations. In panels B and C, the orange arrows indicate wind direction at 500 m. In panel C, wind directions $a \rightarrow b$ and $d \rightarrow c$ are the same; they appear reversed because of the plane flight direction (i.e., pink arrows) that reverses the sequence of the time series of the data.

and strong trade winds (i.e., categories I and II in Table S1). For VOC mixing ratios clustered in category I, strong easterly trade winds parallel to the river dominated (Figure S1A; Table S1; mean speed of 4 m s^{-1}).[41] Relative to the observation site, the river turned to the south at an upwind distance of 35 km so that the study area corresponded to a longitudinally heterogeneous land surface (Figure 1). As shown by the simulations, this setup for strong parallel trade winds (e.g., 4 m s^{-1}) can suppress river winds at the observation site, resulting in reduced VOC transport from the riparian regions and hence lower VOC mixing ratios over the river, in agreement with observations for time periods classified as category I. Conversely, for VOC mixing ratios clustered in category II by meteorology, meaning weak trade winds and strong river winds, higher VOC mixing ratios were observed over the river in both the simulations and the observations. The complex local air circulation cell and the greater instability in it during time periods of category II can also explain the greater variability of VOC mixing ratios during those time periods.

Scenarios in the presence of strong trade winds perpendicular to the river direction were also investigated. Wind speeds were varied stepwise from 0 to 2 m s^{-1}, and the forest−river−forest landscape prescribed in these simulations was the same as that shown in Figure 4A (simulations 9−11, Table S2). For the same wind speeds, the river was then replaced by a hypothetical section of non-emitting forest (simulations 12−14, Table S2). The changes in VOC mixing ratios between these two sets of simulations were used to evaluate the effects of the coupling between perpendicular trade winds and river winds.

The resulting changes, denoted ΔVOC, are plotted in Figure 5 as panels for each wind speed. Blue and red coloring indicates that ΔVOC < 0 and ΔVOC > 0, respectively, for a river in place of a non-emitting forest. In the absence of winds (0 m s^{-1}; Figure 5A), the physics of the river winds reduced the VOC mixing ratios by up to 3 ppb over the riparian forest, which is relative to a background mixing ratio of 4 ppb. The VOC mixing ratios correspondingly increased over the river by 1 to 2 ppb, demonstrating the effects of the river−land circulation. For perpendicular trade winds of 1 and 2 m s^{-1}, these effects weakened (Figure 5B,C). By 2 m s^{-1}, the trade winds dominated the physics, and the river−land circulation was largely suppressed. The maximum ΔVOC was 0.5 ppb. For perpendicular trade winds of 4 m s^{-1}, ΔVOC was

https://doi.org/10.1021/acs.est.1c08460
Environ. Sci. Technol. XXXX, XXX, XXX−XXX

negligible (not shown). Taken together, Figures 3−5 show the importance of both the strength of trade winds and their relative orientation as parallel or perpendicular to the river orientation for defining the extent to which river winds can develop and affect the fate and transport of VOCs in the riparian ecoregion.

An important point of comparison for the UAV-based results of this study is a dataset from an earlier aircraft flight during the GoAmazon2014/5 experiment.[3] That flight was over the same study region in which the boat was deployed for the present study (Figure 6A) and in a similar part of the dry season but in an earlier year (18 September 2014). During the flight, there was afternoon cloud formation over the riverbank upwind of the site (Figure 6B). Clouds were absent, however, both over the river itself and the downwind riverbank (Figure 6B). The regional trade winds at the surface had intermediate strength (2.6 ± 1.0 m s^{-1}, Figure 6C).

Large-eddy simulations suggest that the cloud pattern on that day can be attributed to the direction of the trade winds relative to the river orientation and the intermediate strength of the trade winds (Figure S5). For intermediate winds perpendicular to the river landscape (Figures 6C and S6A), the river−forest circulation cell over the upwind bank of the river was weakened but maintained (Figure S5A). Under this circumstance, the forcing physics by the river−forest landscape and by the trade winds canceled against one another over the upwind riverbank, causing convergence and upward convection (Figure S5B). Likewise, they reinforced one another over the downwind riverbank, allowing for divergence and subsidence. These results are in line with wind observations by the aircraft at 500 m (Figure S6B), showing faster winds over the downwind riverbank (Figure 6A, points b and c) as compared to over the upwind bank (Figure 6A, points a and d). As a result, cloud formation was suppressed over the river and its downwind bank. In the simulation, the effect extended 5 km inland for a river width of 5 km. These results can explain the observed extent of cloud-free air over the downwind riverbank (Figure 6B). A similar interpretation has been made for cloud-free observations over the Tapajós River in the eastern Amazon.[8]

During the aircraft flight, the VOC mixing ratios were continuously measured by mass spectrometry.[42] The isoprene mixing ratio was higher over the upwind bank (points a and d, Figure 6D) compared to that over the downwind bank (points b and c). This profile was also captured in the large-eddy simulation (Figure S5C). Observations for the mixing ratios of other VOCs such as monoterpenes had similar trends (Figure S6C). An overall similar example of these findings for the interplay between river winds and VOC mixing ratios repeated in the dataset for a flight on 30 September 2014 (Figure S7). One implication of this uneven distribution in the VOC mixing ratios over the two banks of the rivers is that different regimes of atmospheric chemistry can develop over each side of the river, resulting in heterogeneity of VOC mixing ratios over the river and the surrounding forests. An additional implication is that caution is warranted for asserting the representativeness regionally or to a particular forest of VOC mixing ratios or emission fluxes based on datasets collected nearby a river when river winds are present.

3.2. River Winds and Atmospheric VOC Oxidation Products. Chemical reactions between VOCs and OH and O_3 in the background atmosphere of the Amazon lead to oxidation products. These secondary products usually have significantly longer atmospheric lifetimes than their VOC precursors. The vertical profiles for the mixing ratios of the secondary products can provide important information when making comparisons to the profiles of the locally emitted VOCs. As one example, methacrolein, which is a product of isoprene oxidation in the atmosphere, has an estimated lifetime against chemical reactions of 10 h under typical conditions of the Amazon. Given this lifetime, without a strong local emission source, methacrolein can become homogeneously mixed in the atmospheric boundary layer across scales of tens of kilometers. In this case, the river winds are not expected to induce atmospheric heterogeneity in its mixing ratio. The measurements of this study supported the above-mentioned expectation (Figures 2 and S2 and Table S4). Even as there was variability explained by river winds in the mixing ratio over the river for the locally emitted isoprene parent compound, there was no statistical difference in the mixing ratio of its oxidation product methacrolein (Figure S2). This corroboration of the expected behavior of secondary products further supports the interpretation of river winds in explaining the observed variability and vertical distribution over the river for the mixing ratios of locally emitted VOCs.

A simulation related to the secondary products was carried out. A hydroxyl radical concentration of 1.0×10^6 molecule cm^{-3} and a chemical yield of 5% for methacrolein from isoprene oxidation were used.[43] The simulated mixing ratios for isoprene over the river, ranging from 0 to 2.5 ppb, were consistent with the observations (Figures 2 and 3C). The river winds in conjunction with the simulated isoprene oxidation increased the mixing ratio of methacrolein from 0.002 to 0.012 ppb over the river (Figure S8). This increase was 50× to 250× smaller than the observed mixing ratios (Figure 2). Those observed mixing ratios represented regional background values because of the atmospheric lifetime of methacrolein and the absence of strong local sources for methacrolein, unlike isoprene. Thus, the incremental contribution of methacrolein from isoprene oxidation to the regional background was negligible over the river, even in the presence of river winds. The implication is that the measured mixing ratios and the absence of atmospheric heterogeneity of VOC oxidation products in the presence of river winds can be explained by the mixing ratio characteristic of the regional background. In contrast, the mixing ratios of the primary VOCs over the river were determined by nearby riparian emission sources during time periods of river winds.[20]

4. ATMOSPHERIC IMPLICATIONS

The influence of river winds on volatile organic transport occurs in the context of an interplay among thermal contrast between the forest and the river, synoptic-scale winds, and atmospheric oxidation chemistry. In the presence of river winds, large-eddy simulations indicated that the VOC concentrations over the river increased. Correspondingly, they decreased over the nearby riparian forest. The simulated maximum in the VOC concentration occurred at mid-heights over the river. The UAV-based datasets of VOC concentrations showed a similar behavior during time periods of river winds, in agreement with the simulations. Analysis of datasets from aircraft measurements at 500 m over the same position in the river during the dry season of 2014 also confirmed the influence of river winds on VOC fate and transport. Although the observations in this study were performed in the dry season of the central Amazon and the analyses focused on biogenic

https://doi.org/10.1021/acs.est.1c08460
Environ. Sci. Technol. XXXX, XXX, XXX−XXX

VOCs, the implications are also applicable to anthropogenic VOCs that originate from urban and industrial sources nearby the rivers[15] and to other seasons (e.g., wet season) of the central Amazon.[16,29]

The observations and analyses reported herein show that the speed and the direction of synoptic-scale trade winds had a strong impact on the possible development of river winds and consequently on VOC concentrations over the river. River winds were most developed, and the VOC concentrations over the river were most significantly altered when trade winds were weak. By comparison, in the presence of strong trade winds parallel to the river orientation, the transport of warm air from an upwind land surface adjacent to the river significantly suppressed the possibility of downwind river winds, as observed in the VOC datasets and as simulated in the study. In the presence of strong trade winds perpendicular to the river orientation, synoptic-scale trade winds instead of river winds dominated the physics and thus also the fate and transport of the VOCs. The influence of river winds also increased with greater thermal contrast in the landscape and greater river width (Section S3).

The Amazon basin is home to many wide rivers. Air circulation induced by river winds alters the dispersion of VOCs and can affect the atmospheric chemistry and lifetime of VOCs. VOCs are critical precursors of ozone and particulate matter. Submicron particulate matter can participate into cloud formation and regulate cloud properties over the river and the forest, playing crucial roles in regional climate. The overall combined sets of observations and simulations here highlight that the linkages between river winds and VOC fate and transport should be carefully considered and included in models of regional chemical transport and climate to better represent the evolution of pollution and biogenic emissions in riparian ecoregions.

■ ASSOCIATED CONTENT

Supporting Information

The Supporting Information is available free of charge at https://pubs.acs.org/doi/10.1021/acs.est.1c08460.

Wind measurements (Section S1), VOC sampling and chemical analysis (Section S2), details and model validation of the DALES (Section S3), summary of UAV wind measurements and VOC collection during the campaign (Table S1), summary of input parameters and results of the large-eddy simulations (Table S2), statistics of VOC mixing ratios for samples collected during the campaign (Table S3), summary of VOC mixing ratios in categories I and II (Table S4), differences in VOC mixing ratios at each height with or without river winds (Table S5), vertical profiles of wind direction for flights in categories I and II (Figure S1), comparison between VOC mixing ratios with and without river winds (Figure S2), large-eddy simulation for the reference case of river winds (Figure S3), influence of river winds on VOC transport for parallel trade winds (Figure S4), transverse distribution of the wind speed and VOC mixing ratio for simulation 10 (Figure S5), aircraft-based observations of VOCs on 18 September 2014 (Figure S6), aircraft-based observations of VOCs on 30 September 2014 (Figure S7), large-eddy simulation for the mixing ratio of methacrolein (Figure S8), example chromatograms for standards and samples (Figure S9), and relationship between the influence length of river winds and thermal contrast in the landscape (Figure S10) (PDF)

■ AUTHOR INFORMATION

Corresponding Author

Scot T. Martin − *School of Engineering and Applied Sciences and Department of Earth and Planetary Sciences, Harvard University, Cambridge, Massachusetts 02138, United States;* orcid.org/0000-0002-8996-7554; Email: scot_martin@harvard.edu

Authors

Jianhuai Ye − *School of Engineering and Applied Sciences, Harvard University, Cambridge, Massachusetts 02138, United States; School of Environmental Science and Engineering, Southern University of Science and Technology, Shenzhen, Guangdong 518055, China;* orcid.org/0000-0002-9063-3260

Carla E. Batista − *School of Technology, Amazonas State University, Manaus, Amazonas 69065-020, Brazil; Post-Graduate Program in Climate and Environment, National Institute of Amazonian Research, Manaus, Amazonas 69060-001, Brazil*

Tianning Zhao − *School of Engineering and Applied Sciences, Harvard University, Cambridge, Massachusetts 02138, United States*

Jesus Campos − *Department of Earth System Science, University of California, Irvine, Irvine, California 92697, United States*

Yongjing Ma − *State Key Laboratory of Atmospheric Boundary Layer Physics and Atmospheric Chemistry, Institute of Atmospheric Physics, Chinese Academy of Sciences, Beijing 100029, China*

Patricia Guimarães − *School of Technology, Amazonas State University, Manaus, Amazonas 69065-020, Brazil; Post-Graduate Program in Climate and Environment, National Institute of Amazonian Research, Manaus, Amazonas 69060-001, Brazil;* orcid.org/0000-0001-8895-7904

Igor O. Ribeiro − *School of Technology, Amazonas State University, Manaus, Amazonas 69065-020, Brazil*

Adan S. S. Medeiros − *School of Technology, Amazonas State University, Manaus, Amazonas 69065-020, Brazil*

Matthew P. Stewart − *School of Engineering and Applied Sciences, Harvard University, Cambridge, Massachusetts 02138, United States*

Jordi Vilà-Guerau de Arellano − *Meteorology and Air Quality Section, Wageningen University, Wageningen 6708 PB, The Netherlands*

Alex B. Guenther − *Department of Earth System Science, University of California, Irvine, Irvine, California 92697, United States*

Rodrigo Augusto Ferreira de Souza − *School of Technology, Amazonas State University, Manaus, Amazonas 69065-020, Brazil; Post-Graduate Program in Climate and Environment, National Institute of Amazonian Research, Manaus, Amazonas 69060-001, Brazil*

Complete contact information is available at: https://pubs.acs.org/10.1021/acs.est.1c08460

https://doi.org/10.1021/acs.est.1c08460
Environ. Sci. Technol. XXXX, XXX, XXX−XXX

Author Contributions

J.Y., C.E.B., A.B.G., R.A.F.d.S., and S.T.M. designed the research; J.Y., C.E.B., T.Z., P.G., I.O.R., A.S.S.M., and M.P.S. conducted UAV flights and sample collection; J.Y., Y.M., and J.V.-G.d.A. carried out the simulations and their interpretation; C.E.B., J.C., and A.B.G. performed the chemical analyses; J.Y. and S.T.M. analyzed the data and wrote the original article; all authors contributed to the data interpretation and paper writing.

Notes

The authors declare no competing financial interest.

Data availability. The numerical experiments were performed using the Dutch Atmospheric Large Eddy Simulation (DALES, version 4.1). It can be downloaded from https://doi.org/10.7910/DVN/X2DAYO. The DALES settings of the reference case (simulation 1, Table S2) are also available at https://doi.org/10.7910/DVN/X2DAYO. Wind information and concentrations of VOCs measured in this study are summarized in Tables S1 and S4.

■ ACKNOWLEDGMENTS

This work was funded by the Division of Atmospheric and Geospace Sciences of the USA National Science Foundation (AGS-1829025 and AGS-1829074). The Brazilian Federal Agency for Support and Evaluation of Graduate Education (CAPES), the Brazilian National Council for Scientific and Technological Development (CNPq), a Senior Visitor Research Grant of the Amazonas State Research Foundation (FAPEAM) (062.00568/2014 and 062.00491/2016), and the Harvard Climate Change Solutions Fund are acknowledged. J.Y. acknowledges support from a postdoctoral fellowship from the Natural Sciences and Engineering Research Council of Canada and a fellowship in Environmental Chemistry from the Dreyfus Foundation. ZOGLAB Microsystem Co. (Hangzhou, China) kindly loaned and operated the UAV6000 and the LWR2500 for the period of measurements. Technical support for the wind measurement during the campaign by Jian Wang and James Sun from ZOGLAB Microsystem Co. is acknowledged.

■ REFERENCES

(1) Martin, S. T.; Artaxo, P.; Machado, L. A. T.; Manzi, A. O.; Souza, R. A. F.; Schumacher, C.; Wang, J.; Andreae, M. O.; Barbosa, H. M. J.; Fan, J.; Fisch, G.; Goldstein, A. H.; Guenther, A.; Jimenez, J. L.; Pöschl, U.; Silva Dias, M. A.; Smith, J. N.; Wendisch, M. Introduction: observations and modeling of the green ocean Amazon (GoAmazon2014/5). *Atmos. Chem. Phys.* **2016**, *16*, 4785−4797.

(2) Pöschl, U.; Martin, S. T.; Sinha, B.; Chen, Q.; Gunthe, S. S.; Huffman, J. A.; Borrmann, S.; Farmer, D. K.; Garland, R. M.; Helas, G.; Jimenez, J. L.; King, S. M.; Manzi, A.; Mikhailov, E.; Pauliquevis, T.; Petters, M. D.; Prenni, A. J.; Roldin, P.; Rose, D.; Schneider, J.; Su, H.; Zorn, S. R.; Artaxo, P.; Andreae, M. O. Rainforest aerosols as biogenic nuclei of clouds and precipitation in the Amazon. *Science* **2010**, *329*, 1513−1516.

(3) Martin, S. T.; Artaxo, P.; Machado, L.; Manzi, A. O.; Souza, R. A. F.; Schumacher, C.; Wang, J.; Biscaro, T.; Brito, J.; Calheiros, A.; Jardine, K.; Medeiros, A.; Portela, B.; de Sá, S. S.; Adachi, K.; Aiken, A. C.; Albrecht, R.; Alexander, L.; Andreae, M. O.; Barbosa, H. M. J.; Buseck, P.; Chand, D.; Comstock, J. M.; Day, D. A.; Dubey, M.; Fan, J.; Fast, J.; Fisch, G.; Fortner, E.; Giangrande, S.; Gilles, M.; Goldstein, A. H.; Guenther, A.; Hubbe, J.; Jensen, M.; Jimenez, J. L.; Keutsch, F. N.; Kim, S.; Kuang, C.; Laskin, A.; McKinney, K.; Mei, F.; Miller, M.; Nascimento, R.; Pauliquevis, T.; Pekour, M.; Peres, J.; Petäjä, T.; Pöhlker, C.; Pöschl, U.; Rizzo, L.; Schmid, B.; Shilling, J. E.; Dias, M. A. S.; Smith, J. N.; Tomlinson, J. M.; Tóta, J.; Wendisch, M. The Green Ocean Amazon Experiment (GoAmazon2014/5) observes pollution affecting gases, aerosols, clouds, and rainfall over the rain forest. *Bull. Am. Meteorol. Soc.* **2017**, *98*, 981−997.

(4) Hess, L. L.; Melack, J. M.; Affonso, A. G.; Barbosa, C.; Gastil-Buhl, M.; Novo, E. M. L. M. Wetlands of the lowland Amazon basin: extent, vegetative cover, and dual-season inundated area as mapped with JERS-1 synthetic aperture radar. *Wetlands* **2015**, *35*, 745−756.

(5) Gibbs, R. J. Water chemistry of the Amazon River. *Geochim. Cosmochim. Acta* **1972**, *36*, 1061−1066.

(6) dos Santos, M. J.; Silva Dias, M. A. F.; Freitas, E. D. Influence of local circulations on wind, moisture, and precipitation close to Manaus City, Amazon Region, Brazil. *J. Geophys. Res.: Atmos.* **2014**, *119*, 13233−13249.

(7) Santos, M. J.; Medvigy, D.; Silva Dias, M. A. F.; Freitas, E. D.; Kim, H. Seasonal flooding causes intensification of the river breeze in the central Amazon. *J. Geophys. Res.: Atmos.* **2019**, *124*, 5178−5197.

(8) Silva Dias, M. A. F.; Silva Dias, P. L.; Longo, M.; Fitzjarrald, D. R.; Denning, A. S. River breeze circulation in eastern Amazonia: observations and modelling results. *Theor. Appl. Climatol.* **2004**, *78*, 111−121.

(9) Fitzjarrald, D. R.; Sakai, R. K.; Moraes, O. L. L.; Cosme de Oliveira, R.; Acevedo, O. C.; Czikowsky, M. J.; Beldini, T. Spatial and temporal rainfall variability near the Amazon-Tapajós confluence. *J. Geophys. Res.: Biogeosci.* **2008**, *113*, G00B11.

(10) Lu, L.; Denning, A. S.; da Silva-Dias, M. A.; da Silva-Dias, P.; Longo, M.; Freitas, S. R.; Saatchi, S. Mesoscale circulations and atmospheric CO_2 variations in the Tapajós Region, Pará, Brazil. *J. Geophys. Res.: Atmos.* **2005**, *110*, D21102.

(11) Bracho-Nunez, A.; Knothe, N. M.; Costa, W. R.; Maria Astrid, L. R.; Kleiss, B.; Rottenberger, S.; Piedade, M. T. F.; Kesselmeier, J. Root anoxia effects on physiology and emissions of volatile organic compounds (VOC) under short-and long-term inundation of trees from Amazonian floodplains. *SpringerPlus* **2012**, *1*, 9.

(12) Jardine, K.; Chambers, J.; Holm, J.; Jardine, A.; Fontes, C.; Zorzanelli, R.; Meyers, K.; De Souza, V.; Garcia, S.; Gimenez, B.; Piva, L.; Higuchi, N.; Artaxo, P.; Martin, S.; Manzi, A. Green leaf volatile emissions during high temperature and drought stress in a Central Amazon rainforest. *Plants* **2015**, *4*, 678−690.

(13) Pegoraro, E.; Abrell, L.; Van Haren, J.; Barron-Gafford, G.; Grieve, K. A.; Malhi, Y.; Murthy, R.; Lin, G. The effect of elevated atmospheric CO2 and drought on sources and sinks of isoprene in a temperate and tropical rainforest mesocosm. *Glob. Change Biol.* **2005**, *11*, 1234−1246.

(14) Gentine, P.; Massmann, A.; Lintner, B. R.; Hamed Alemohammad, S.; Fu, R.; Green, J. K.; Kennedy, D.; Vilà-Guerau de Arellano, J. Land−atmosphere interactions in the tropics—a review. *Hydrol. Earth Syst. Sci.* **2019**, *23*, 4171−4197.

(15) Zhao, T.; Ye, J.; Ribeiro, I. O.; Ma, Y.; Hung, H.-M.; Batista, C. E.; Stewart, M. P.; Guimarães, P. C.; Vilà-Guerau de Arellano, J.; de Souza, R. A. F.; Guenther, A. B.; Martin, S. T. River winds and pollutant recirculation near the Manaus city in the central Amazon. *Commun. Earth Environ.* **2021**, *2*, 205.

(16) de Oliveira, A. P.; Fitzjarrald, D. R. The Amazon river breeze and the local boundary layer: I. Observations. *Bound.-Layer Meteorol.* **1993**, *63*, 141−162.

(17) De Oliveira, A. P.; Fitzjarrald, D. R. The Amazon river breeze and the local boundary layer: II. Linear analysis and modelling. *Bound.-Layer Meteorol.* **1994**, *67*, 75−96.

(18) Miller, S. T. K.; Keim, B. D.; Talbot, R. W.; Mao, H. Sea breeze: structure, forecasting, and impacts. *Rev. Geophys.* **2003**, *41*, 1011.

(19) Trebs, I.; Mayol-Bracero, O. L.; Pauliquevis, T.; Kuhn, U.; Sander, R.; Ganzeveld, L.; Meixner, F. X.; Kesselmeier, J.; Artaxo, P.; Andreae, M. O. Impact of the Manaus urban plume on trace gas mixing ratios near the surface in the Amazon Basin: Implications for the NO-NO_2-O_3 photostationary state and peroxy radical levels. *J. Geophys. Res.: Atmos.* **2012**, *117*, D05307.

(20) Batista, C. E.; Ye, J.; Ribeiro, I. O.; Guimarães, P. C.; Medeiros, A. S. S.; Barbosa, R. G.; Oliveira, R. L.; Duvoisin, S.; Jardine, K. J.; Gu,

https://doi.org/10.1021/acs.est.1c08460
Environ. Sci. Technol. XXXX, XXX, XXX−XXX

D.; Guenther, A. B.; McKinney, K. A.; Martins, L. D.; Souza, R. A. F.; Martin, S. T. Intermediate-scale horizontal isoprene concentrations in the near-canopy forest atmosphere and implications for emission heterogeneity. *Proc. Natl. Acad. Sci. U.S.A.* **2019**, *116*, 19318−19323.
(21) Guimarães, P.; Ye, J.; Batista, C.; Barbosa, R.; Ribeiro, I.; Medeiros, A.; Souza, R.; Martin, S. T. Vertical profiles of ozone concentration collected by an unmanned aerial vehicle and the mixing of the nighttime boundary layer over an amazonian urban area. *Atmosphere* **2019**, *10*, 599.
(22) McKinney, K. A.; Wang, D.; Ye, J.; de Fouchier, J.-B.; Guimarães, P. C.; Batista, C. E.; Souza, R. A. F.; Alves, E. G.; Gu, D.; Guenther, A. B.; Martin, S. T. A sampler for atmospheric volatile organic compounds by copter unmanned aerial vehicles. *Atmos. Meas. Tech.* **2019**, *12*, 3123−3135.
(23) Guimarães, P.; Ye, J.; Batista, C.; Barbosa, R.; Ribeiro, I.; Medeiros, A.; Zhao, T.; Hwang, W.-C.; Hung, H.-M.; Souza, R.; Martin, S. T. Vertical profiles of atmospheric species concentrations and nighttime boundary layer structure in the dry season over an urban environment in central Amazon collected by an unmanned aerial vehicle. *Atmosphere* **2020**, *11*, 1371.
(24) Ye, J.; Batista, C. E.; Guimarães, P. C.; Ribeiro, I. O.; Vidoudez, C.; Barbosa, R. G.; Oliveira, R. L.; Ma, Y.; Jardine, K. J.; Surratt, J. D.; Guenther, A. B.; Souza, R. A. F.; Martin, S. T. Near-canopy horizontal concentration heterogeneity of semivolatile oxygenated organic compounds and implications for 2-methyltetrols primary emissions. *Environ. Sci.: Atmos.* **2021**, *1*, 8−20.
(25) Küchler, I. L.; Miekeley, N.; Forsberg, B. R. A contribution to the chemical characterization of rivers in the Rio Negro Basin, Brazil. *J. Braz. Chem. Soc.* **2000**, *11*, 286−292.
(26) Stropp, J.; Sleen, P. V. d.; Assunção, P. A.; Silva, A. L. d.; Steege, H. T. Tree communities of white-sand and terra-firme forests of the upper Rio Negro. *Acta Amazonica* **2011**, *41*, 521−544.
(27) National Aeronautics and Space Administration (U.S.). The Earth Observing System Data and Information System Worldview. https://worldview.earthdata.nasa.gov (accessed August 12, 2021).
(28) Li, Y.; Liu, B.; Ye, J.; Jia, T.; Khuzestani, R. B.; Sun, J. Y.; Cheng, X.; Zheng, Y.; Li, X.; Wu, C.; Xin, J.; Wu, Z.; Tomoto, M. A.; McKinney, K. A.; Martin, S. T.; Li, Y. J.; Chen, Q. Unmanned aerial vehicle measurements of volatile organic compounds over a subtropical forest in China and implications for emission heterogeneity. *ACS Earth Space Chem.* **2021**, *5*, 247−256.
(29) Medeiros, A. S. S.; Ribeiro, I. O.; Morais, M. V. B.; Andreoli, R. V.; Martins, J. A.; Martins, L. D.; Batista, C. E.; Guimarães, P. C.; Martin, S. T.; Souza, R. A. F. River breezes for pollutant dispersion in GoAmazon2014/5. *Atmos. Chem. Phys. Discuss.* **2018**, 1−28.
(30) Ma, Y.; Ye, J.; Ribeiro, I. O.; Vilà-Guerau de Arellano, J.; Xin, J.; Zhang, W.; Souza, R. A. F. d.; Martin, S. T. Optimization and Representativeness of Atmospheric Chemical Sampling by Hovering Unmanned Aerial Vehicles Over Tropical Forests. *Earth Space Sci.* **2021**, *8*, No. e2020EA001335.
(31) Heus, T.; van Heerwaarden, C. C.; Jonker, H. J. J.; Pier Siebesma, A.; Axelsen, S.; van den Dries, K.; Geoffroy, O.; Moene, A. F.; Pino, D.; de Roode, S. R.; Vilà-Guerau de Arellano, J. Formulation of the Dutch Atmospheric Large-Eddy Simulation (DALES) and overview of its applications. *Geosci. Model Dev.* **2010**, *3*, 415−444.
(32) Vilà-Guerau de Arellano, J.; Kim, S. W.; Barth, M. C.; Patton, E. G. Transport and chemical transformations influenced by shallow cumulus over land. *Atmos. Chem. Phys.* **2005**, *5*, 3219−3231.
(33) Vilà-Guerau de Arellano, J.; Patton, E. G.; Karl, T.; van den Dries, K.; Barth, M. C.; Orlando, J. J. The role of boundary layer dynamics on the diurnal evolution of isoprene and the hydroxyl radical over tropical forests. *J. Geophys. Res.: Atmos.* **2011**, *116*, D07304.
(34) Vilà-Guerau de Arellano, J.; Wang, X.; Pedruzo-Bagazgoitia, X.; Sikma, M.; Agustí-Panareda, A.; Boussetta, S.; Balsamo, G.; Machado, L. A. T.; Biscaro, T.; Gentine, P.; Martin, S. T.; Fuentes, J. D.; Gerken, T. Interactions between the Amazonian rainforest and cumuli clouds: a large-eddy simulation, high-resolution ECMWF, and observational intercomparison study. *J. Adv. Model. Earth Syst.* **2020**, *12*, No. e2019MS001828.
(35) Ma, Y.; Ye, J.; Ribeiro, I. O.; Vilà-Guerau de Arellano, J.; Xin, J.; Zhang, W.; Souza, R. A. F.; Martin, S. T. Optimization and representativeness of atmospheric chemical sampling by hovering unmanned aerial vehicles over tropical forests. *Earth Space Sci.* **2021**, *8*, No. e2020EA001335.
(36) Alves, E. G.; Jardine, K.; Tota, J.; Jardine, A.; Yãnez-Serrano, A. M.; Karl, T.; Tavares, J.; Nelson, B.; Gu, D.; Stavrakou, T.; Martin, S.; Artaxo, P.; Manzi, A.; Guenther, A. Seasonality of isoprenoid emissions from a primary rainforest in central Amazonia. *Atmos. Chem. Phys.* **2016**, *16*, 3903−3925.
(37) Yáñez-Serrano, A. M.; Nölscher, A. C.; Bourtsoukidis, E.; Gomes Alves, E.; Ganzeveld, L.; Bonn, B.; Wolff, S.; Sa, M.; Yamasoe, M.; Williams, J.; Andreae, M. O.; Kesselmeier, J. Monoterpene chemical speciation in a tropical rainforest: variation with season, height, and time of dayat the Amazon Tall Tower Observatory (ATTO). *Atmos. Chem. Phys.* **2018**, *18*, 3403−3418.
(38) Greenberg, J. P.; Guenther, A. B.; Pétron, G.; Wiedinmyer, C.; Vega, O.; Gatti, L. V.; Tota, J.; Fisch, G. Biogenic VOC emissions from forested Amazonian landscapes. *Glob. Change Biol.* **2004**, *10*, 651−662.
(39) Kesselmeier, J.; Kuhn, U.; Wolf, A.; Andreae, M. O.; Ciccioli, P.; Brancaleoni, E.; Frattoni, M.; Guenther, A.; Greenberg, J.; De Castro Vasconcellos, P.; de Oliva, T.; Tavares, T.; Artaxo, P. Atmospheric volatile organic compounds (VOC) at a remote tropical forest site in central Amazonia. *Atmos. Environ.* **2000**, *34*, 4063−4072.
(40) Guenther, A. B.; Jiang, X.; Heald, C. L.; Sakulyanontvittaya, T.; Duhl, T.; Emmons, L. K.; Wang, X. The model of emissions of gases and aerosols from nature version 2.1 (MEGAN2.1): An extended and updated framework for modeling biogenic emissions. *Geosci. Model Dev.* **2012**, *5*, 1471−1492.
(41) Martin, S. T.; Andreae, M. O.; Artaxo, P.; Baumgardner, D.; Chen, Q.; Goldstein, A. H.; Guenther, A.; Heald, C. L.; Mayol-Bracero, O. L.; McMurry, P. H.; Pauliquevis, T.; Pöschl, U.; Prather, K. A.; Roberts, G. C.; Saleska, S. R.; Silva Dias, M. A.; Spracklen, D. V.; Swietlicki, E.; Trebs, I. Sources and properties of Amazonian aerosol particles. *Rev. Geophys.* **2010**, *48*, RG2002.
(42) Shilling, J. E.; Pekour, M. S.; Fortner, E. C.; Artaxo, P.; de Sá, S.; Hubbe, J. M.; Longo, K. M.; Machado, L. A. T.; Martin, S. T.; Springston, S. R.; Tomlinson, J.; Wang, J. Aircraft observations of the chemical composition and aging of aerosol in the Manaus urban plume during GoAmazon 2014/5. *Atmos. Chem. Phys.* **2018**, *18*, 10773−10797.
(43) Mao, J.; Paulot, F.; Jacob, D. J.; Cohen, R. C.; Crounse, J. D.; Wennberg, P. O.; Keller, C. A.; Hudman, R. C.; Barkley, M. P.; Horowitz, L. W. Ozone and organic nitrates over the eastern United States: Sensitivity to isoprene chemistry. *J. Geophys. Res.: Atmos.* **2013**, *118*, 11256−11268.

https://doi.org/10.1021/acs.est.1c08460
Environ. Sci. Technol. XXXX, XXX, XXX−XXX